Vol-3, Issue-6 PP. 452-465 ISSN: 2394-5788

GLOBAL JOURNAL OF ADVANCED RESEARCH
(Scholarly Peer Review Publishing System)

TREATMENT OF AQUEOUS SOLUTION OF NITRATE CONTENT BY USING NATURAL MIXTURE OF KAOLINITE-QUARTZ-BOEHMITE

Marie Anne Etoh & Charles Melea Kede
University of Douala/Faculty of Sciences,
Analytical and structural mineral chemistry laboratory,
PO BOX: 24157 Douala,
Cameroon

Pierre G Tchiéta, Daniel J David Dina & S Boh-Lere
University of Douala/Faculty of Sciences,
Analytical and structural mineral chemistry laboratory,
PO BOX: 24157 Douala,
Cameroon

ABSTRACT
The adsorption kinetics of NO_3^- ions from aqueous solution onto clay fractionated from Nkongsamba (Cameroon) soil based on particle size (≤53µm) has been investigated. Spectroscopic studies including FTIR, elemental analysis (EA), XRPD, and SEM were used for its characterization. Batch studies were carried out to investigate the effect of contact time and initial concentrations of NO_3^- ions on kinetics adsorption. Kinetic studies showed a rapid adsorption during the first thirty minutes. Application of pseudo first order, pseudo second order and intraparticle diffusion model equations showed that the experimental results are well expressed by pseudo second order kinetic equation. Maximum adsorption capacity, calculated from well fitted Langmuir equation, is 29.585mg/g. Verification of intra-particle diffusion model showed that intra-particle diffusion could be one of the rate determining steps but pseudo second order mechanism is predominant. Overall adsorption process appears to be controlled by more than one step.

Keywords: Adsorption; Kinetic; Equilibrium; Clays; Nitrates ions.

1. INTRODUCTION
Nitrate is found in moderate concentrations in most of the natural waters. It occurs naturally due to the degradation of nitrogen-containing compounds from natural sources as soil, bedrock and organic materials [1]. Nitrate is also present as natural constituent of plants. Together with sulfates, nitrates are main components of acid rains [2]. However, the largest loading of nitrate originates from anthropogenic sources, which mostly result from excessive application of nitrate-based chemical fertilizers in agricultural activities [3,4] and from many industrial processes [5,6]. The other most common sources of nitrate are overflowing septic tanks [6,7] livestock, domestic wastes effluents, pesticides and herbicides that are used in industrial agriculture [7], the wastes of the production of explosives[1], decomposition of decaying organic matters buried in the ground [6] and the plantation of leguminosae crops which fix atmospheric nitrogen in the form of nitrate [8].

All these products can be converted to nitrate by biochemical oxidation. The nitrite ion occurs as intermediate during the

GLOBAL JOURNAL OF ADVANCED RESEARCH
(Scholarly Peer Review Publishing System)

biodegradation which happens through a series of bacterial reactions collectively known as nitrification. In the nitrification process bacteria degrade nitrogen-containing compounds and release ammonia. Then, some bacteria such as Nitrosom onas oxidize the released ammonia to nitrite which is converted to nitrate by other bacteria such as Nitrobacter [10].

Nitrates are extremely soluble in water and can move easily through soil into the drinking water supply [6] and when their concentrations become excessive in water sources they cause several health and environmental problems.
Nitrate in water has low toxicity, but may be converted via micro bacteria or in vivo reduction to nitrites [2]. Nitrites transform hemoglobin into methaemoglobin by oxidation of ferrous iron (Fe^{2+}) in hemoglobin to ferric form (Fe^{3+}) preventing or reducing the ability of blood to transport oxygen. Such a condition is described as methaemoglobinanemia which is dangerous especially in infants (so-called “blue-baby syndrom”) [11]. In addition, the reaction between nitrite and secondary or tertiary amines may result in the formation of carcinogenic, mutagenic and teratogenic N-nitrosocompounds (N-nitrosoamines) [11,12] which may cause cancer of the alimentary canal[13, 14]. In adults, high amounts of nitrate may cause abdominal pain, blood in stool and urine, weakness, mental depression, dyspepsia, headache [15], diarrhea, vomiting, diabetes, hypertension, respiratory tract infections and changes in the immune system [15]. The high concentrations of nitrate in water causes a phenomenon known as “Eutrophication”, which means an excessive growth of the algae in water which consumes the oxygen gas dissolved in water causing fish death[16].

For these reasons, removal of nitrate from water is a necessity. To limit the risk to human health from nitrate in drinking water, the World Health Organization (WHO) has set the maximum acceptable concentration of NO_3^- to be 50 mg/L [17]. At high nitrate concentrations, water must be treated to meet regulated concentrations. The following treatment processes have been studied or applied to remove nitrate from drinking water: biological denitrification [6, 16], ion exchange [15], reverse osmosis [3, 4] electrodialysis [8],chemical denitrification [1], chemical reduction [7] and adsorption [15].

Clays attract attention due to the heterogeneity of their surfaces and some have been found to possess the ability to sorbs ions from solutions and release them later, when the conditions change [12]. There are about thirty different types of "pure" clays but most natural clays are mixtures of these different types, along with other weathered minerals [17]. Studies have shown that natural clay is an appropriate adsorbent for heavy metal removal due to its efficiency, low cost and availability [17]. The adsorption capacity of natural clay to remove nitrate ions in aqueous solutions is due to their high surface area and exchange capacities [16] including the presence of negative charges on the clay mineral structure which can attract positively charged metal ions [18].

2. MATERIALS AND METHODS

2.1. Chemicals

Stock solution of nitrate was prepared by dissolving 1.631 g of KNO_3 of analytical reagent grade (Merck) in 1 L of double-distilled water. The test solutions were prepared by diluting stock solution to the desired concentrations. Experiments were conducted with nitrate concentrations in the ranges of 20-100 mg L^{-1}.

2.2. Materials

The natural clays used in this study was mined from a subtropical wetland soil in Cameroon ((Littoral Region), West Africa. For this type of clay material, the cation exchange capacity (CEC) = 13.2 meq/100 g was considered. The clays were washed several times with distilled and deionized water after which they were completely dispersed in water. After 17 h at rest, the dispersed particles were centrifuged for one hour at 2400 rpm. The size r of the clay particles obtained was between 0.5 and 2 μm.

2.3. Characterization of the materials

The purity of the activated natural clay samples was tested by IR spectral analysis. An IR transmittance spectrum of the ground samples was obtained in the 4000 to 400 cm^{-1} range on a PerkinElmer Spectrum Two spectrometer (UK).

To confirm the purity of the activated natural clay samples, x-ray diffraction (XRD) spectra were obtained. Analysis involved the identification and semi quantification of the characteristic peaks of the minerals present. The XRD diffractograms presented in this study were recorded using a Bruker D8 Discover X-Ray diffractrometer (XRD) (UK) from Bruker (Germany) with a D5000 Ni-

GLOBAL JOURNAL OF ADVANCED RESEARCH
(Scholarly Peer Review Publishing System)

filtered CuK and an α radiation of 1.5406 Å. Scans of natural clay samples with both randomly and preferred orientation were taken over a range from 2θ = 10° to 100°at scanning speeds of 0.03°/5 s. The XRD patterns were collected using a Cu Kα radiation (1, 5406 Å) source (40 keV, 40 mA). The scans were performed at room temperature in 2θ steps of 0.02°, using open sample holders. The phases were identified using Bruker Diffract Plus evaluation software, distributed by the International Centre for Diffraction Data (ICDD).

The clay was examined with a scanning electron microscope (SEM) coupled to an X-ray (EDX) analyzer. N_2–physisorption experiments (adsorption isotherms for pore size distribution (PSD) and surface area) were conducted with a Micromeritics ASAP 2010 (USA) surface area and porosity analyzer. Analyses of adsorption and desorption of nitrogen were conducted at 195 °C. Before the experiments, the sample was degassed at 200 °C overnight. Total surface areas were determined by applying the BET equation.

Field emission scanning electron microscopy (FE-SEM) and energy-dispersive X-ray (EDX) analysis were conducted to observe the surface morphology of the clay. The samples were gold coated to improve their conductivity to obtain good images. Elemental analysis (EA) for the carbon (C), nitrogen (N), oxygen (O), sulfur (S) and metal content of the various samples was carried out with the aid of the energy dispersive-X-ray device. The instrument used to obtain SEM images of the samples and EDS spectra was a JEOL JSM-7600F field emission scanning electron microscope, 800 mm^2, X-Max coupled to a silicon drift energy dispersive X-ray detector (SDD) (Oxford Instruments Ltd, UK).

2.4. Equilibrium adsorption studies

A constant mass of adsorbent (0.2 g) was weighed into 250 ml glass bottles and contacted with 50 ml of NO_3^- solutions of different initial concentration. The bottles were sealed and placed in a shaker until equilibrium was reached. Upon equilibration, samples of 4–5 ml were withdrawn from the flasks and the adsorbents were separated from the solution by centrifugation (REMI make) at 2000 rpm for 10 minutes, and analyzed to determine the residual equilibrium liquid-phase NO_3^- concentration. The sorption equilibrium data of NO_3^-on clay was analyzed using Freundlich and Langmuir isotherm models**.** Freundlich isotherm equation $x/m = k_f C^{1/n}$ can be written in the linear form as given below (1).

Where x/m (mg/g) and C_e(mg/L) are the equilibrium concentrations of NO_3^- in the adsorbed and liquid phases. K_F and n are the Freundlich constants that are related to the sorption capacity and intensity, respectively. Freundlich constants K_F and n can be calculated from the slope and intercept of the linear plot, with log (x/m) versus logC_e.

The Langmuir sorption isotherm equation $\frac{x}{m} = \frac{Q_{\max} K_L C_e}{1 + k_L C_e}$ on linearization becomes (2):

$$\frac{C_e}{Q_e} = \frac{1}{K_L Q_{\max}} + \frac{1}{Q_{\max}} C_e \qquad (3)$$

Where Q_{max} is the adsorption capacity (mg/g) when all adsorption sites are occupied, C_e is the equilibrium concentration of NO_3^-, and the Langmuir constant K_L (L/mg) is derived from the ratio of the adsorption rate constant to the desorption rate constant.

2.5. Kinetic studies

Kinetic adsorption data were analyzed following pseudo-first-order kinetic model:

$$\frac{dq_t}{dt} = k_1 (q_e - q_t) \qquad (4)$$

Where q_e and q_t refer to the amount of NO_3^- ions adsorbed (mg/g) at equilibrium and at any time, t (h), respectively, and k_1 is the equilibrium rate constant of pseudo-first-order sorption (1/h). Integration of Eq. (3) for the boundary conditions t=0 to t and q_t=0 to q_t, gives

GLOBAL JOURNAL OF ADVANCED RESEARCH
(Scholarly Peer Review Publishing System)

$$\log\frac{q_e}{(q_e-q_t)}=\log q_e-\frac{k_1 t}{2.303} \quad (5)$$

Eq. (4)can be rearranged to give (5)

$$\log(q_e-q_t)=\log q_e-\frac{k_1 t}{2.303} \quad (6)$$

The pseudo second-order model was well-fitted to the NO_3^- sorption data on the minerals. The rate equation for the second-order model can be expressed as:

$$\frac{dq_t}{dt}=k_2(q_e-q_t)^2 \quad (7)$$

Where k_2 is the equilibrium rate constant of pseudo-second-order adsorption (g/mg min). Integrating Eq. (7) for the boundary condition t=0 to t and q_t=0 to q_t, gives (7):

$$\frac{1}{(q_e\_q_t)}=\frac{1}{q_t}+k_2.t \quad (8)$$

Which is the integrated rate law for a pseudo-second-order reaction. Eq. (7) can be rearranged to obtain a linear form (9):

$$\left(\frac{t}{q_t}\right)=\left(\frac{t}{q_e}\right)+\left[\left(\frac{1}{k_2.q_e^2}\right)\right] \quad (10)$$

where, q_t and q_e (mg/g) are the amount of NO_3^-sorbed on the mineral at time t and at equilibrium, respectively and k_2 ($g.mg^{-1}.min^{-1}$) is the second-order rate constant.

2.6. Adsorption mechanism

In the model developed by Weber and Morris, the rate of intra-particle diffusion is a function of $t^{1/2}$ and can be defined by Eq. (9) as follows:

$$q=f\left(\frac{D_t}{r_p^2}\right)^{1/2}=k_w t^{1/2} \quad (11)$$

Where r_p is particle radius, D_t is the effective diffusivity of solutes within the particle, and Kw intraparticular diffusion rate. Kw values can be obtained by linearizing the curve q = f ($t^{1/2}$).

3. RESULTS AND DISCUSSIONS

3.1. Characterisation of clay

3.1.1. XRD analysis

Table 1 shows the mineral composition of the clay used. The main constituent of the crude clay is SiO_2 (56.48 w.t.%), Al_2O_3 is the next main constituent (22.39 w.t.%) followed by notable amounts of Fe_2O_3 (7.483 w.t.%), K_2O(1.671 w.t.%), TiO_2 (1.505 w.t.%) and MgO (1.483 w.t.%).

GLOBAL JOURNAL OF ADVANCED RESEARCH
(Scholarly Peer Review Publishing System)

Table 1: Chemical composition of clay material from Nkongsamba

Major elements	SiO_2	Al_2O_3	Fe_2O_3	K_2O	TiO_2	MgO	P_2O_5	ZrO_2	CaO	Cr_2O_3	V_2O_5	MnO	SrO	Nb_2O_5	Rb_2O	ZnO	LOI
W_t(%)	56.48	22.39	7.483	1.671	1.505	1.483	0.091	0.055	0.029	0.017	0.016	0.013	0.011	0.008	0.008	0.006	8.65

The X-rays powder diffractogramms of the crude clay (Fig 1) shows the presence of three clayey minerals with some impurities: (i) Kaolinite, identified by its ray at 7.22Å,3.58 Å and 2.56 Å in crude clay: (ii) Quartz recognized for its typical rays at 4.25 Å, 3.35 Å, 2.43 Å and 1.82Å (iii): Boehmite known for the displaying a dool at 6.11 Å and 2.56 Å[19 ,20].

The results presented in the table 2 show the mineralogical composition of the crude clay material. Whole rock comprises quartz (79.19%), kaolinite (26.86%) and boehmite (4.87%).

Table 2: mineralogical composition of clay from Nkongsamba

mineral	Formula	Y-Scale
Quartz	SiO_2	79.19
Kaolinite	$Al_4(OH)_8(Si_4O_{10})$	26.86
Boehmite	$AlO_{1.06}(OH)_{0.94}$	4.87

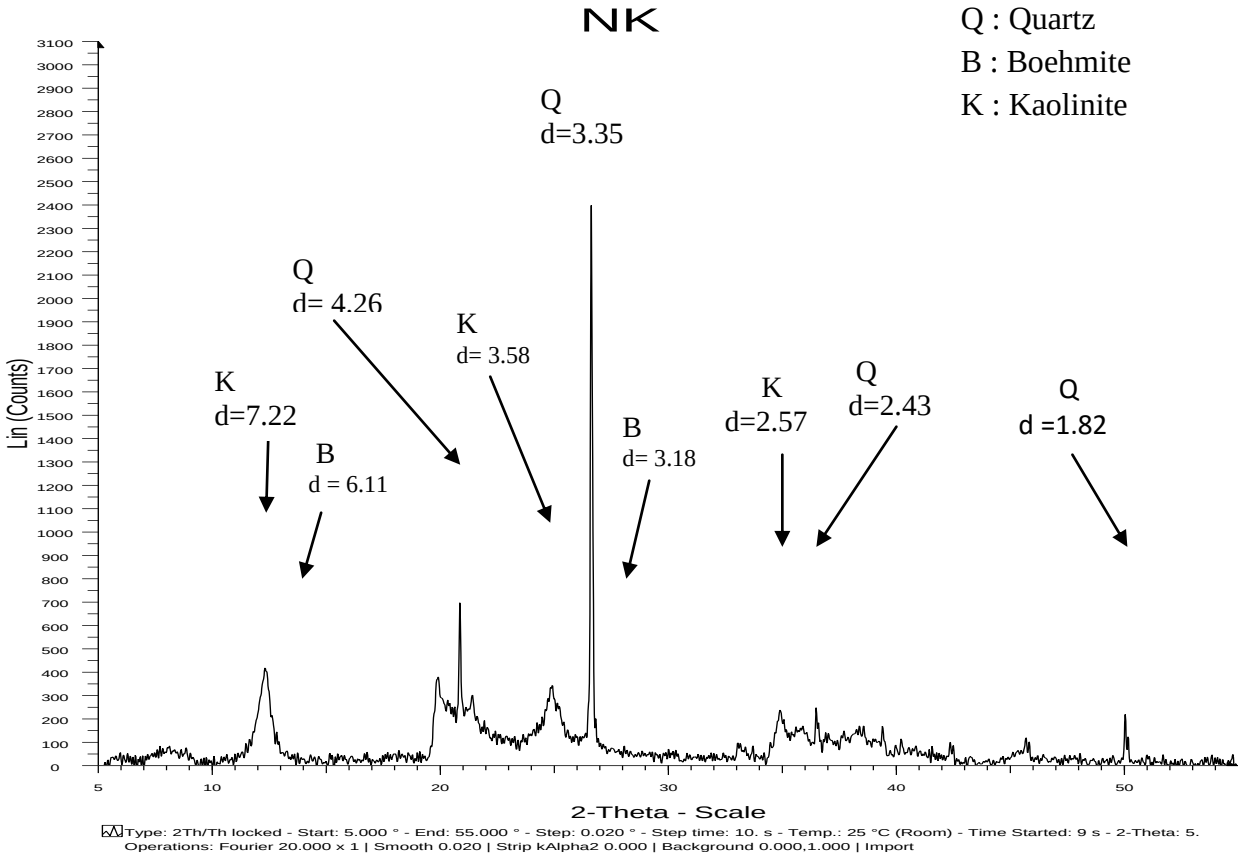

Fig.1. X-ray diffraction patterns of the natural clay.

GLOBAL JOURNAL OF ADVANCED RESEARCH
(Scholarly Peer Review Publishing System)

3.1.2. Fourier transform-infrared spectroscopy (FTIR)

The FTIR spectrum of the clay is shown in Fig 2. The frequency absorption band at 3692.3 cm^{-1}(OH-Al out-of-plane), 3692.3, 3650.96 and 3620.23 cm^{-1} (OH-Al in-plane), 997.80$cm^{-1}$and 908.47 cm^{-1} indicate the presence of OH-Al groups [14].
Moreover, few weak intensity peaks rises at 3363.61 cm^{-1} and 3259.21 cm^{-1} showing non hydrogen bonded hydroxyl groups [15].
On one hand, peaks appearing between (1400 and 1500 cm^{-1}) depicts the presence of alkyl groups (CH_2-CH_3 and CH_3 [15, 21].
The bands appearing at 908.47 cm^{-1} and 639.92cm^{-1} indicates the presence of boehmite.
The bands observed at 468.88 and 540 cm^{-1} can be attributed to vibrations due to deformation of Si-O and Si-O-Al bonds, respectively [22, 23].

The bands appearing at 1025.50 and 1113.88 cm^{-1} are ascribed to the formation of Si-O bond, characteristic of aluminosilicate [23]. The additional peak at 695.45 cm^{-1} indicates the presence of Al-OH and Si-O [24].

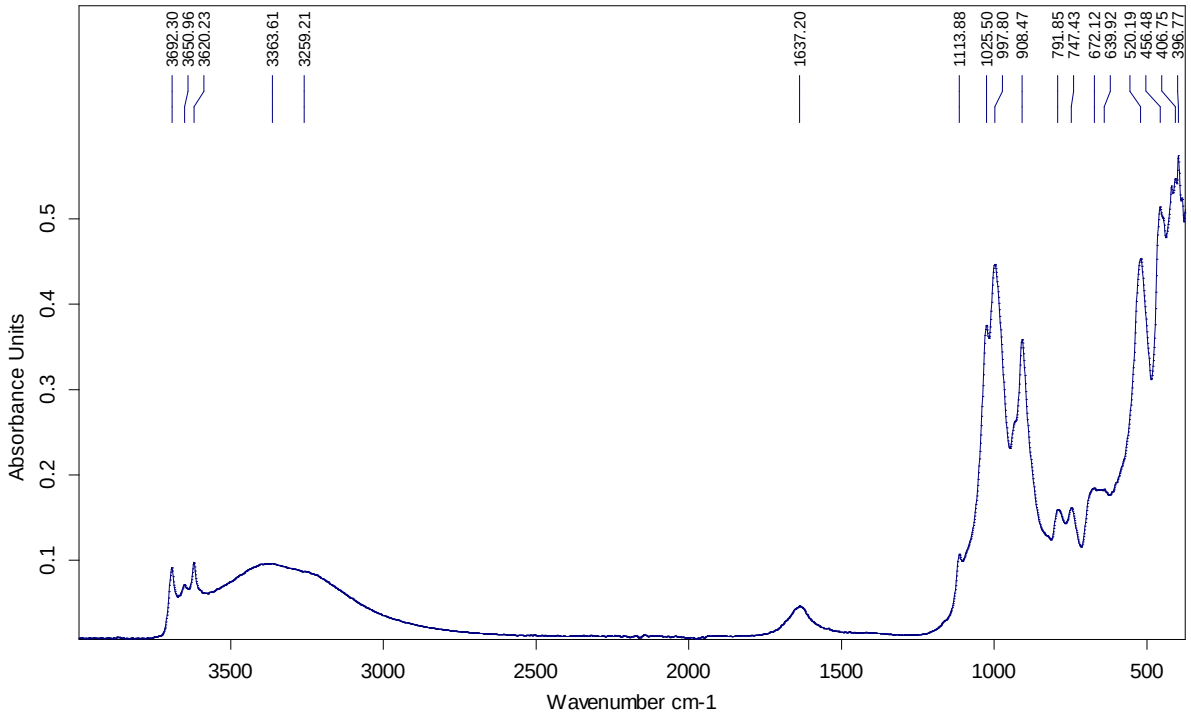

Fig. 2.FTIR spectrum of a sample clay studied

3.1.3. Specific surface area and SEM micrographs of clay observations

The surface area of clay was determined by nitrogen (N_2) adsorption-desorption isotherms at (77K) using an automated gas sorption system (Micromeritics, QUAN- TACHROME instrument).The specific surface area was calculated by the Brunauer-Emmett-Teller (BET) method, it is equal to 32.52 m^2/g.

Scanning Electron Microscopy (SEM) technique was employed to observe the surface physical morphology of clay (Fig 3).

GLOBAL JOURNAL OF ADVANCED RESEARCH
(Scholarly Peer Review Publishing System)

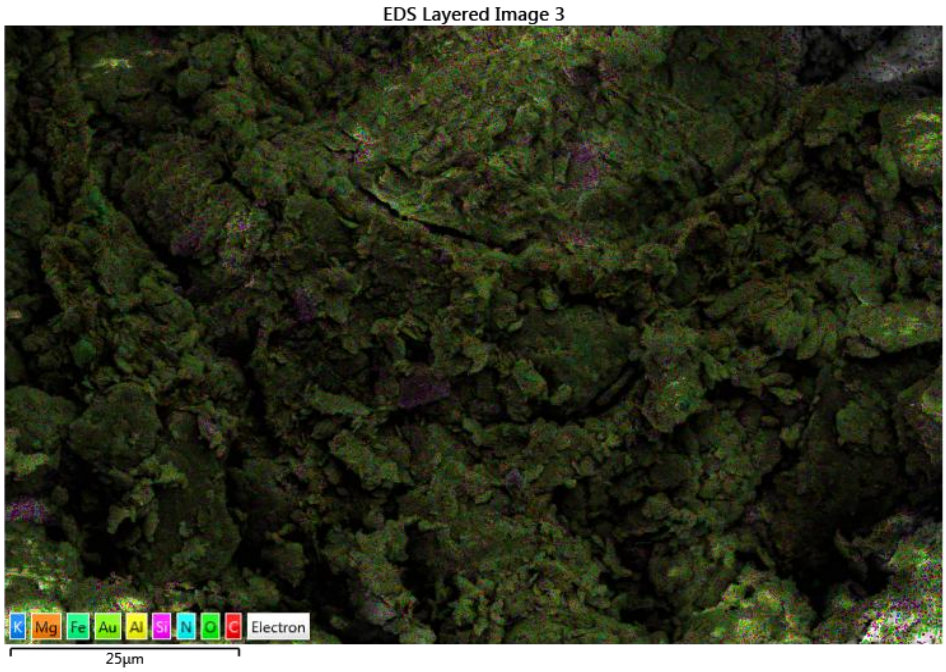

Fig 3: SEM micrograph of clay at sizes of 100 µm, 20 µm and 10 µm

The morphological aspects of the clay were determined by Scanning Electron Microscopy (SEM) measurements using an FEG Quanta 450 electron microscope equipped with an EDS
Bruker QUANTAX system coupled to the SEM microscope, using an acceleration voltage of 2 kV. The porosity of the surface is clearly visible. The scanning electron micrograph of the fig3 shows the typical regular shapes of the clay particles. The powder is rich in porous particles with fibrous morphology and also of angular-shaped particles of quartz, Kaolinite and Bohemite.

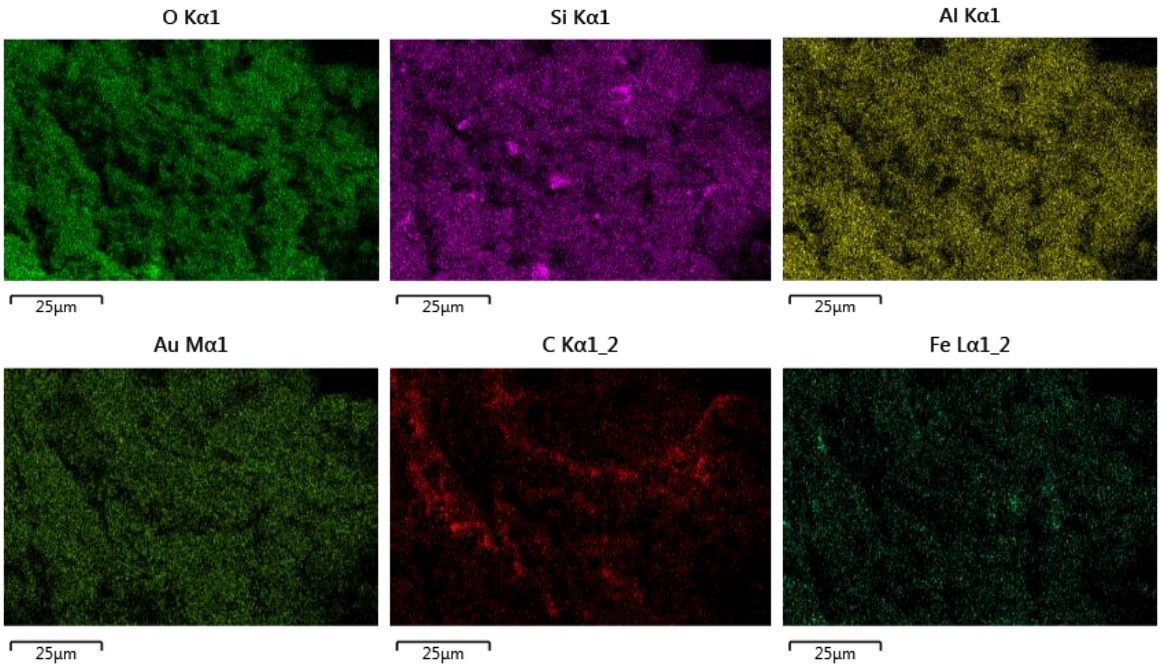

GLOBAL JOURNAL OF ADVANCED RESEARCH
(Scholarly Peer Review Publishing System)

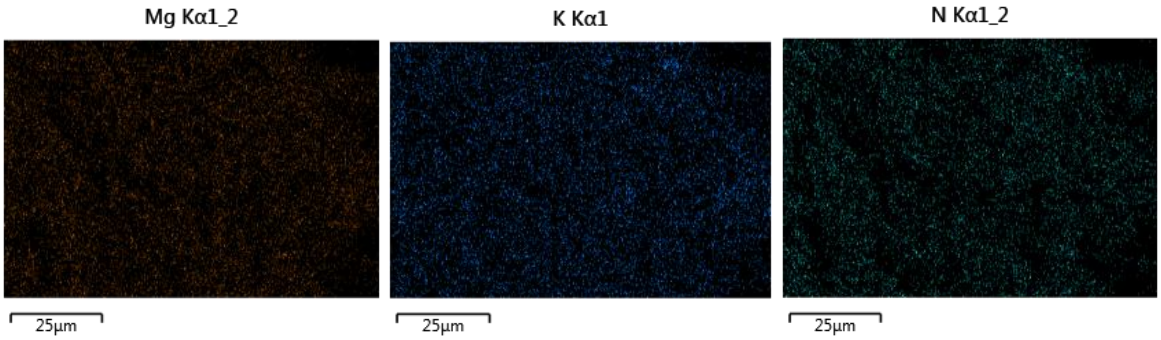

Fig 4: SEM micrograph of the characteristic colors of the elemental compositions of the clay

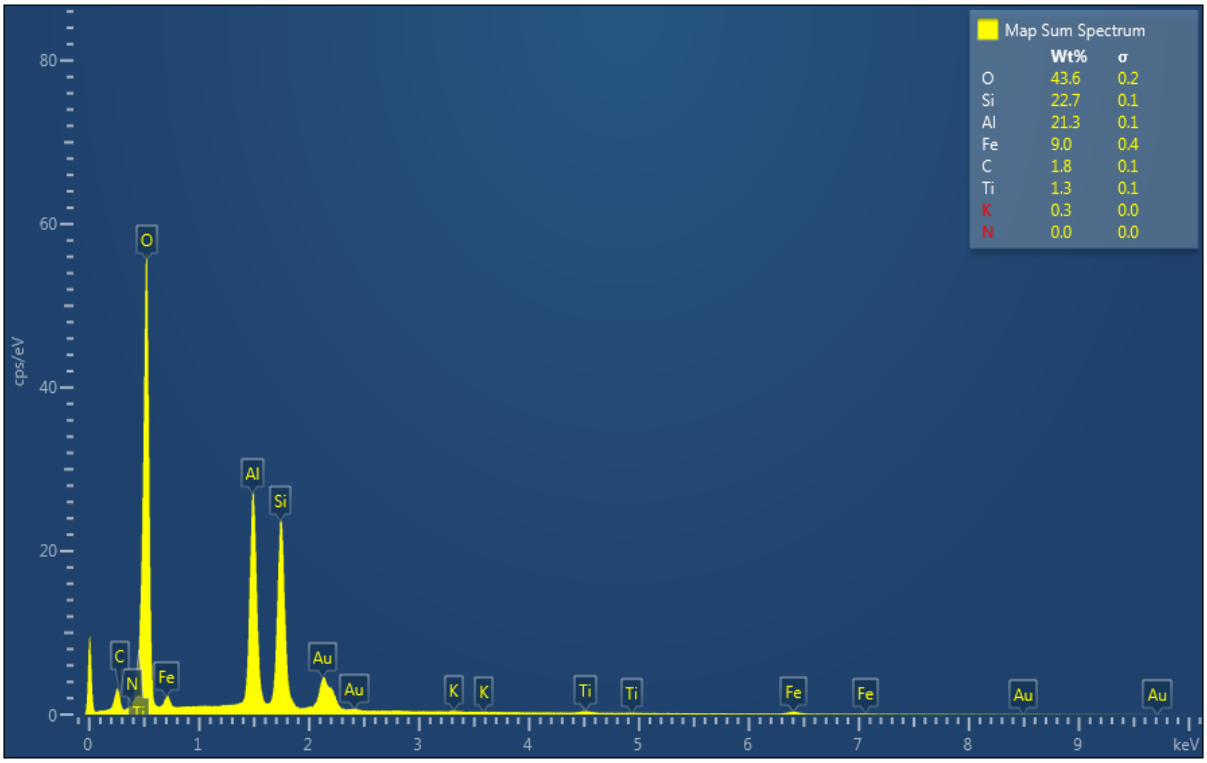

Fig. 5.EDS of a sample clay sample MARV4 showing abundance of certain metals (Al and Si are typically present in clay minerals of this type)

Additionally, EDS elemental spectra of a few spots on the samples were taken for determining the elemental compositions fig 5. We present here the representative images and spectra of the samples as well as the characteristic colors of the various elements represented by fig 4 found on our clay.

3.2 Effects of Contact Time and Initial Concentration of NO_3^-

The effect of contact time on batch adsorption of initial $\mathbf{NO_3^-}$ concentration ranged from 20 to 100 ppm at room temperature is shown in Fig 6. The amount of adsorption increases rapidly in the beginning and then gradually increases to reach an equilibrium value in 60 minutes. The increase in uptake capacity of the adsorbent with increasing $\mathbf{NO_3^-}$ concentration may be due to higher probability of

GLOBAL JOURNAL OF ADVANCED RESEARCH
(Scholarly Peer Review Publishing System)

collision between NO_3^- ions and adsorbent particles. The variation in the extent of adsorption may also be due to the fact that initially all sites on the surface of adsorbent were vacant and the solute concentration gradient was relatively high. Consequently, the extent of NO_3^- uptake decreases significantly with the increase of contact time, which is depending on the decrease in the number of vacant sites on the surface. This data is important because equilibrium time is one of the parameters for economic feasibility studies for in wastewater treatment plant application [25, 26]. According to these results; the agitation time was fixed at 2h for the rest of the batch experiments to make sure that equilibrium was attained.

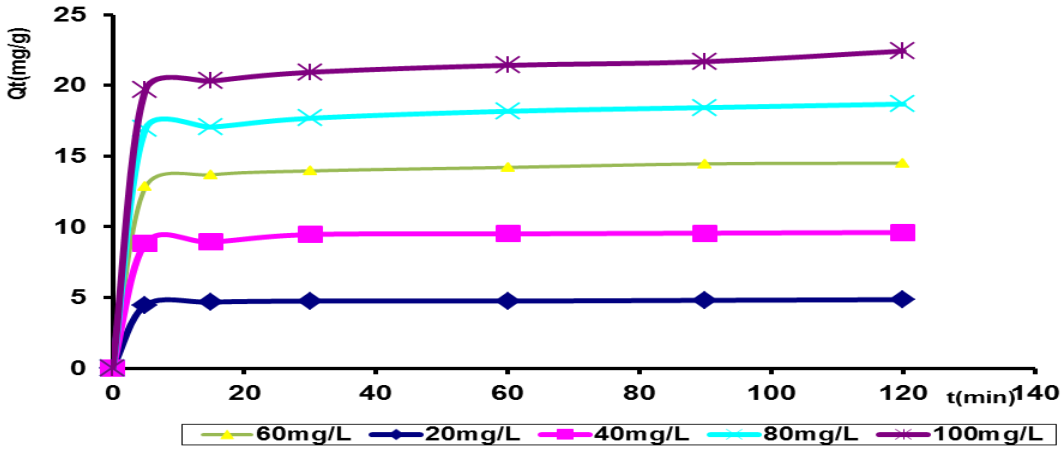

Fig.6. Effect of agitation time and initial concentration of NO_3^- on the adsorption of NO_3^-clay concentration, 0.2g/50 mL.)

3.3 Equilibria Isotherms

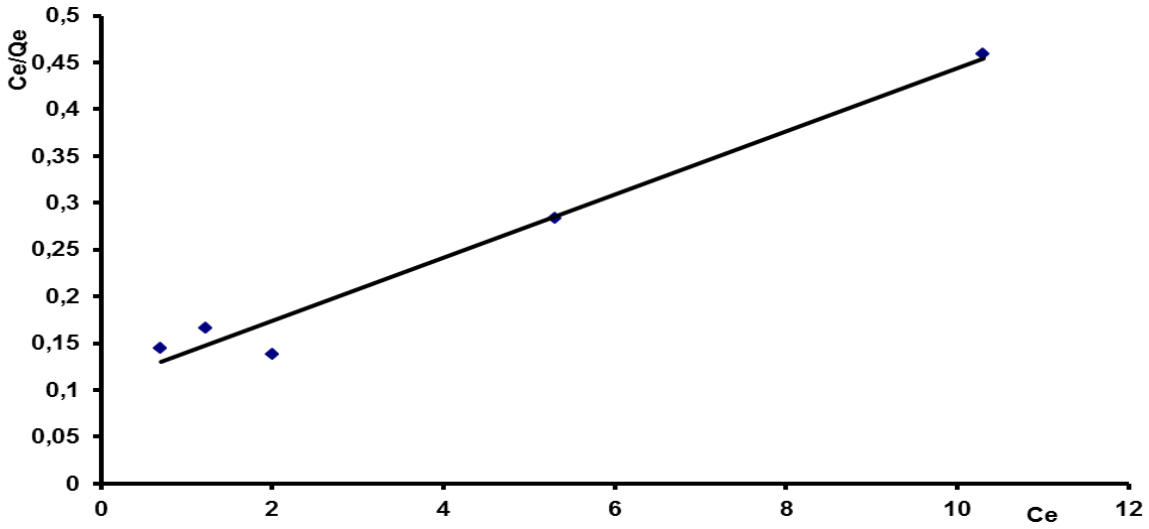

Fig 7. Langmuir isotherm for cadmium adsorption onto clay at room temperature

GLOBAL JOURNAL OF ADVANCED RESEARCH
(Scholarly Peer Review Publishing System)

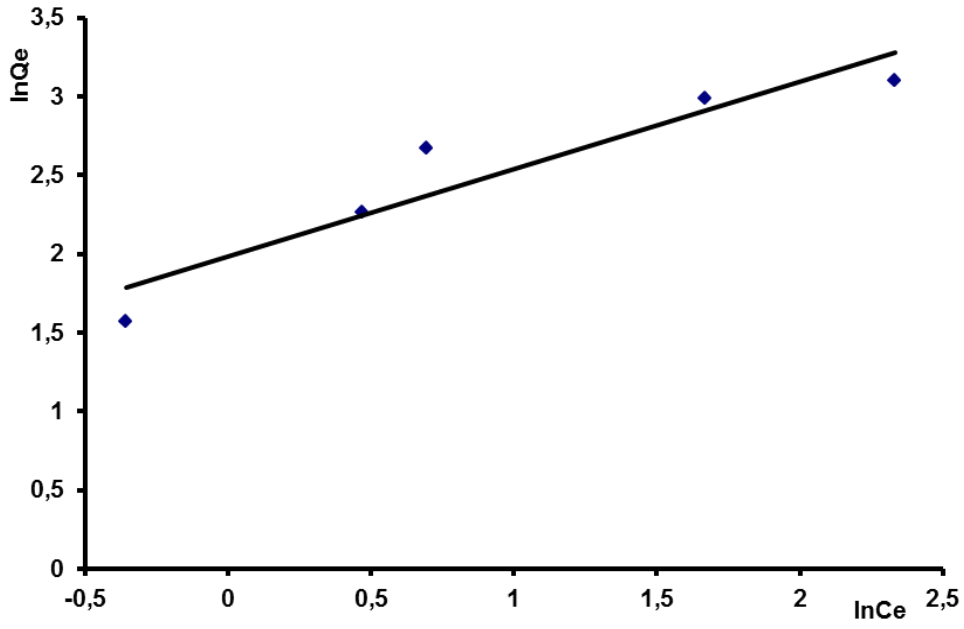

Fig 8.Freundlich isotherm for nitrate ions adsorption onto clay at room temperature

The analysis of the isotherm data is important to develop an equation which accurately represents the results and could beused for designing purposes. The sorption data was analysed in terms of Freundlich and Langmuir isotherm models. The fitted constants for Freundlich and Langmuir models along with regression coefficients are summarised in Table 3. The Freundlich and Langmuir isotherms are shown graphically in Figs. 8 and 7.As can be seen from isotherms and regression coefficients, the fit is better with Langmuir model than Freundlich model. The Langmuir constants Q_{max} and K_L were 29.585 mg/g and 0.317 for nitrate ions.

Table 3.Isotherm parameters for NO_3^- adsorption onto clay

	Q_{max}(mg/g)	K_L (L/mg)	R^2
Langmuir	29.585	0.317	0.975
Freundlich	K_f (mg/g)	N	R^2
	0.686	1.802	0.884

3.4 Kinetic Studies

In order to investigate the kinetics of adsorption of NO_3^-, the Lagergren-first-order model and Ho's pseudo-second-order model [27, 28, 29] were used. The values of the parameters and the correlation coefficients obtained using linear regression by origin version 7.0 at four concentrations are listed in Table 4. Adsorption equation obtained and the fitting of the kinetic models are illustrated in Fig.9-10. It was found that the fitting to Ho's pseudo-second-order model gave the highest values of correlation coefficients more accurately than the other two models investigated. Therefore, Ho's pseudo-second-order model could be used for the prediction of the kinetics of adsorption of NO_3^-on clay.

GLOBAL JOURNAL OF ADVANCED RESEARCH
(Scholarly Peer Review Publishing System)

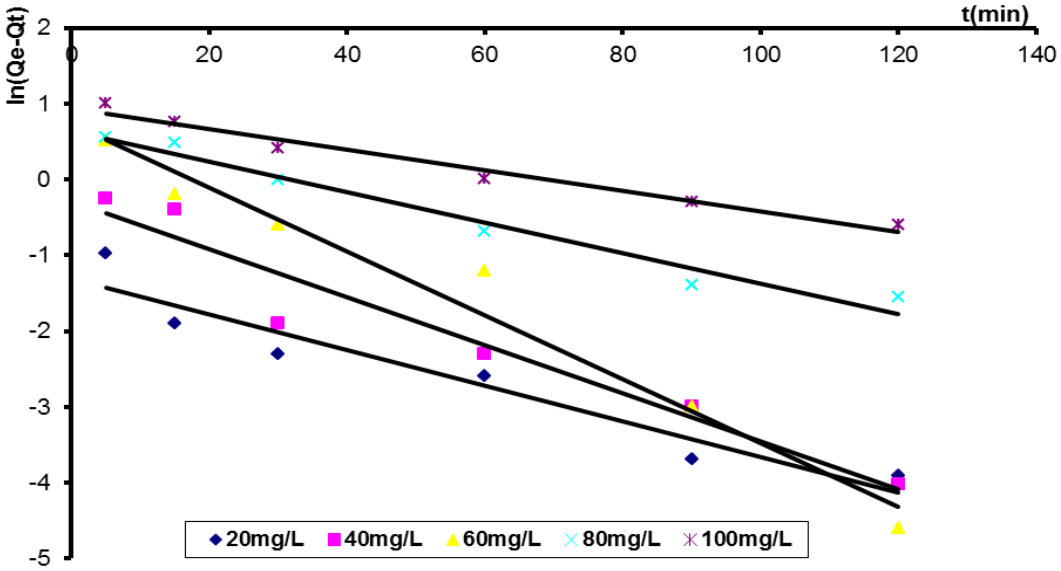

Fig.9. Pseudo-first-orderkinetics for adsorption of NO_3^-onto clay

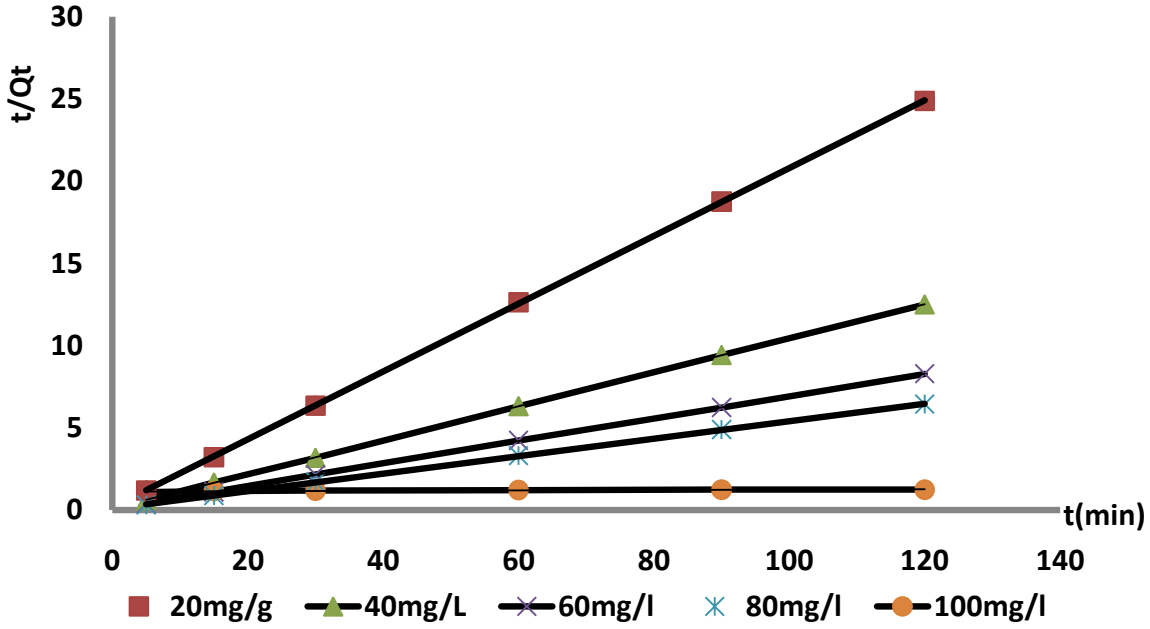

Fig. 10. Pseudo-second-orderkinetics for adsorption of NO_3^-onto clay

GLOBAL JOURNAL OF ADVANCED RESEARCH
(Scholarly Peer Review Publishing System)

Table 4. Kinetic parameters for NO_3^- adsorption onto clay

Model	Lagergren		2nd order		Intraparticle diffusion	
	$K_1(min^{-1})$	R^2	$K_{2app}(g.mg^{-1}.min^{-1})$	R^2	K_w	R^2
20 ppm	0.052	0.922	0.261	0.999	0.406	0.858
40 ppm	0.072	0.940	0.110	0.989	0.291	0.912
60 ppm	0.097	0.972	0.066	0.997	0.134	0.969
80 ppm	0.046	0.967	0.033	0.999	0.131	0.759
100ppm	0.031	0.971	0.008	0.970	0.055	0.637

3.5 Adsorption Mechanism

Due to stirring there is a possibility of transport of nitrate species from the bulk into pores of the clay as well as adsorption at outer surface of the clay. The rate-limiting step may be either adsorption or intra particle diffusion. As they act in series, the slower of the two, will be the rate determining step. The possibility of nitrate species to diffuse into the particles of clay was tested with Weber-Morris equation [27].

In order to study the diffusion process, batch adsorption experiments were carried out with clay at ambient temperature with initial nitrate concentration. The results obtained are presented in the table 4 and graphically shown in the fig 11. The rate constants K_w for intraparticle diffusion for various initial concentrations of nitrate solution, for clay were determined from the slope of respective plots. It is evident from the graph that, the plots were straight lines but the y-intercept of the plots were nonzero (not passing through the origin) thus indicating that intraparticle diffusion is not the sole rate limiting factor for the adsorption of nitrate onto clay. It also indicates that the mechanism of nitrate removal on clay is complex and both surface adsorption as well as intraparticle diffusion contributes to the rate determining step [28].

The values of K_w in table 4 for clay used in this study show the increase in K_w with the increase in nitrate concentration. It can be related to concentration diffusion [29].

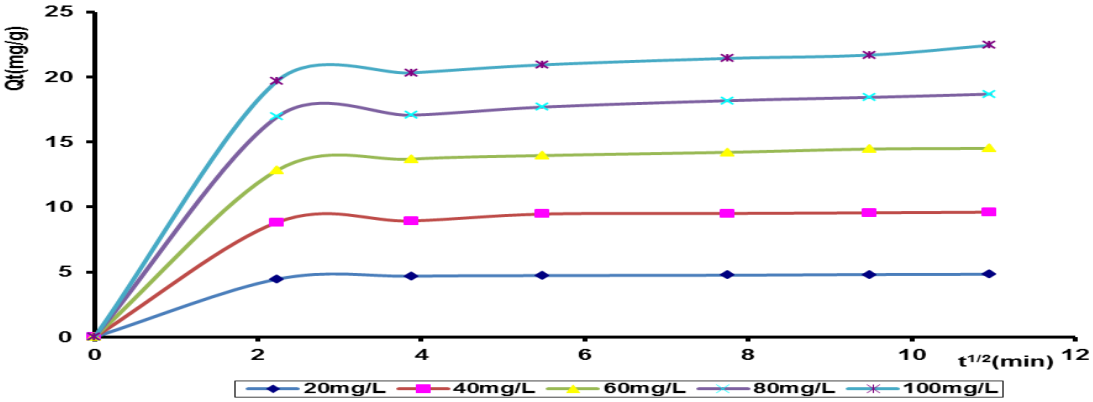

Fig 11.Plot of the intra-particle diffusion model for the adsorption of NO_3^-

GLOBAL JOURNAL OF ADVANCED RESEARCH
(Scholarly Peer Review Publishing System)

4. CONCLUSION

In this study, the removal of NO_3^- from aqueous solution by this clay, as a natural available adsorbent, was investigated. Adsorption capacity of adsorbent increased with increasing initial concentration of NO_3^-. The equilibrium uptake was increased with the increasing of the initial concentration of NO_3^- in solution. The Langmuir and Freundlich adsorption models were used to describe the equilibrium between adsorbed NO_3^- on the adsorbent (Q_{ads}) and NO_3^- in solution (C_e) at room temperature. The equilibrium data were best described by the Langmuir isotherm model. The results show that the natural clay is an excellent adsorbent for the used NO_3^-. Finally, this local clay can be used as an effective natural adsorbent for the economic treatment of water.

5. REFERENCES

[1] Afkhami. A., Madrakian. T. and Karimi. Z., (2007). The effect of acid treatment of carbon cloth on the adsorption of nitrite and nitrate ions**,** J. Hazardous Materials**, 144,** 427-431

[2] Mikuska. P. and Vecera. Z., (2003). Simultaneous determination of nitrite and nitrate in water by chemiluminescent flow-injection analysis**,** Analytica Chimica Acta, 495**,** 225-232

[3] Rocca. C. D., Belgiorno. V. and Meric, S., (2007). Overview of in-situ applicable nitrate removal processes**,** Desalination, 204, 46-62.

[4] Ayyasamy. P.M., Rajakumar. S., Sathishkumar. M., waminathanc. K.S., Shanthi. K., Lakshmanaperumalsamye. P., Lee. S., (2009). Nitrate removal from synthetic medium and groundwater with aquatic macrophytes, Desalination, 242, 286-296.

[5] Öztürkand. N., Köse. T.E., (2008). A kinetic study of nitrite adsorption onto sepiolite and powdered activated carbon, Desalination, 223, 174-179.

[6] Mishra, P.C., Patel.R.K., (2009). Use of agricultural waste for the removal of nitrate-nitrogen from aqueous medium, J. Environmental Management, 90, 519-522.

[7] Okafor, P.N. and Ogbonna, U.I., (2003). Nitrate and nitrite contamination of water sources and fruit juices marketed in South-Eastern Nigeria, J. Food Composition and Analysis,16, 213-218

[8] Batheja, K., Sinha, A.K. and Seth, G., (2009). Studies on water treatment for removal of nitrate, Asian J. Exp.Sci., 23:(1), 61-66.

[9] Grommena, R., Hauteghem, I.V., Wambeke, M.V and Verstraete, W. (2002). An improved nitrifying enrichment to remove ammonium and nitrite from fresh water aquaria systems, Aquaculture, 211, 115-124.

[10] Melchert, W.R., Infante, C.M.C. and Rocha, F.R.P., (2007). Development and critical comparison of greener flow procedures for nitrite determination in natural waters, Microchemical Journal, 85, 209-213.

[11] Lohumi, N., Gosain, S., Jain, A., Gupta, V. K, Verma, K. K., (2004). Determination of nitrate in environmental water samples by conversion into nitrophenol sand solid phase extraction−spectrophotometry, liquid chromatography or gas chromatography–mass spectrometry, Analytica Chimica Acta, 505: (2), 231-237.

[12] Valle, C. J. D., Corzo, M. G., Villegas, J. P. and Serrano, V. G., (2005). Study of cherry stones as raw material in preparation of carbonaceous adsorbents, Analytical and Applied Pyrolysis, 73: (1), 59-67

[13] Borello, E.; Zecchina, A.; Castelli, M. Ann. Chim. **1963**, 53, 690.

GLOBAL JOURNAL OF ADVANCED RESEARCH
(Scholarly Peer Review Publishing System)

[14] Babel, S. and Kurniawan, T.A., 2003. Low-cost adsorbents for heavy metals uptake from contaminated water: a review. J. Hazard. Mater., 97: 219-243.

[15] Jalali, R., Ghafourian, H., Asef, Y., Davarpanah, S.J. and Sepehr, S., 2002. Removal and recovery of lead using nonliving biomass of marine algae. J. Hazard. Mater., 92: 253-262.

[16] Zaini, M.A.A., Amano, Y. and Machida, M., 2010. Adsorption of heavy metals onto activated carbons derived from polyacrylonitrile fiber. J. Hazard. Mater., 180: 552-560. 353.

[17] World Health Organization, Guidelines for Drinking-Water Quality: Incorporating, First Addendum. Vol. 1, Recommendations (2006), 3rd edition, WHO, NLM classification: WA 675.

[18] Babel, S. and Kurniawan, T.A., 2003. Low-cost adsorbents for heavy metals uptake from contaminated water:a review. J. Hazard. Mater., 97: 219-243.

[19] Kim, D.S., 2004. Adsorption characteristics of Fe(III) and Fe(III)-NTA complex on granular activated carbon. J. Hazard. Mater. 106: 67-84.

[20] Senthilkumar, R., Vijayaraghavan, K., Thilakavathi, M., Iyer, P.V.R. and Velan, M., 2006. Seaweeds for the remediation of wastewaters contaminated with zinc(II) ions. J. Hazard. Mater., 136: 791-799

[21] Kede, C.M., Etoh, M.A., Ndibewu, P.P., Ngomo, H.M. and Ghogomu, P.M., 2014. Equilibria and kinetic studies on the adsorption of cadmium onto Cameroonian wetland clays. British J. Applied Sci. Technol., **4**(7), 1070–1088.

[22] Kaewsarn, P., 2002. Biosorption of copper (II) from aqueous solutions by pre-treated biomass of marine algae Padinasp. Chemosphere, 47: 1081-1085.

[23] Mathialagan, T. and Viraraghavan, T., 2002. Adsorption of cadmium from aqueous solutions by perlite. J. Hazard. Mater., 94: 291-303.

[24] Veli, S. and Alyuz, B., 2007. Adsorption of copper and zinc from aqueous solutions by using natural clay.J.Hazard. Mater., 149: 226-233.

[25] Bhattacharyya, K.G. and Gupta, S.S., 2008. Kaolinite and montmorillonite as adsorbents for Fe(III), Co(II) and Ni(II) in aqueous medium. Appl. Clay Sci., 41: 1-9.

[26] Forestier, L.L., Muller, F., Villieras, F. and Pelletier, M., 2010. Textural and hydration properties of a synthetic montmorillonite compared with a natural Na-exchanged clay analogue. Appl. Clay Sci., 48: 18-25

[27] Ivan, S. and Velimin P., 1998. The colloid and surface chemistry of clays in natural waters. CCACAA, 71:1061-1074.

[28] Cuevas, J., S. Leguey, A. Garralon, M.R. Rastrero, J.R. Procopio, M.T. Sevilla, N.S. Jimenez, R.R. Abad and A. Garrido, 2009. Behavior of kaolinite and illite-based clays as landfill barriers. Appl. Clay Sci., 42: 497-509.

[29] Kadirvelu, K., Faur-Brasquet, C. and Le Cloiree, P., (2000). Removal of Cu(II), Pb(II) and Ni(II) by adsorption onto activated carbon cloths. Langmuir, 16: 8604-8409.

[30] Kadirvelu, K., Kavipriya, S., Karthika, C., Radhika, M., Vennilamani, N. and Pattabhi, S., (2003). Utilization of various agricultural wastes for activated carbon preparation and application for the removal of dyes and metal ions from aqueous solutions. Bioresource Technol., 87: 129-132.